Discovery of biased orientation of human DNA motif sequences affecting enhancer-promoter interactions and transcription of genes

Naoki Osato[1*]

[1]Department of Bioinformatic Engineering, Graduate School of Information Science and Technology, Osaka University, Osaka 565-0871, Japan

[*]Corresponding author

E-mail address: naokiosato11@gmail.com, nosato@ist.osaka-u.ac.jp

Abstract

Chromatin interactions have important roles for enhancer-promoter interactions (EPI) and regulating the transcription of genes. CTCF and cohesin proteins are located at the anchors of chromatin interactions, forming their loop structures. CTCF has insulator function limiting the activity of enhancers into the loops. DNA binding sequences of CTCF indicate their orientation bias at chromatin interaction anchors – forward-reverse (FR) orientation is frequently observed. DNA binding sequences of CTCF were found in open chromatin regions at about 40% - 80% of chromatin interaction anchors in Hi-C and in situ Hi-C experimental data. Though the number of chromatin interactions was about seventy thousand in Hi-C at 50kb resolution, about twenty millions of chromatin interactions were recently identified by HiChIP at 5kb resolution. It has been reported that long range of chromatin interactions tends to include less CTCF at their anchors. It is still unclear what proteins are associated with chromatin interactions.

To find DNA binding motif sequences of transcription factors (TF), such as CTCF, and repeat DNA sequences affecting the interaction between enhancers and promoters of genes and their expression, first I predicted TF bound in enhancers and promoters using DNA motif sequences of TF and experimental data of open chromatin regions in monocytes and other cell types, which were obtained from public and commercial databases. Second, transcriptional target genes of each TF were predicted based on enhancer-promoter association (EPA). EPA was shortened at the genomic locations of FR or reverse-forward (RF) orientation of DNA motif sequence of a TF,

which were supposed to be at chromatin interaction anchors and acted as insulator sites like CTCF. Then, the expression levels of the transcriptional target genes predicted based on the EPA were compared with those predicted from only promoters.

Total 369 biased orientation of DNA motifs (232 FR and 178 RF orientation, the reverse complement sequences of some DNA motifs were also registered in databases, so the total number was smaller than the number of FR and RF) affected the expression level of putative transcriptional target genes significantly in $CD14^+$ monocytes of four people in common. The same analysis was conducted in $CD4^+$ T cells of four people. DNA motif sequences of CTCF, cohesin and other transcription factors involved in chromatin interactions were found to be a biased orientation. Transposon sequences, which are known to be involved in insulators and enhancers, showed a biased orientation. The biased orientation of DNA motif sequences tended to be co-localized in the same open chromatin regions. Moreover, for 36 – 95% of FR and RF orientations of DNA motif sequences, EPI predicted from EPA that were shortened at the genomic locations of the biased orientation of DNA motif sequence were overlapped with chromatin interaction data (Hi-C and HiChIP) significantly more than other types of EPAs.

Keywords: transcriptional target genes, gene expression, transcription factors, enhancer, enhancer-promoter interactions, chromatin interactions, CTCF, cohesin, open chromatin regions, co-location of transcription factors, homodimer, heterodimer, complex

Background

Chromatin interactions have important roles for enhancer-promoter interactions (EPI) and regulating the transcription of genes. CTCF and cohesin proteins are located at the anchors of chromatin interactions, forming their loop structures. CTCF has insulator function limiting the activity of enhancers into the loops (Fig. 1A). DNA binding sequences of CTCF indicate their orientation bias at chromatin interaction anchors – forward-reverse (FR) orientation is frequently observed (de Wit et al. 2015; Guo et al. 2015). About 40% - 80% of chromatin interaction anchors of Hi-C and in situ Hi-C experiments include DNA binding motif sequences of CTCF. Though the number of chromatin interactions was about seventy thousand in Hi-C at 50kb resolution (Javierre et al. 2016), about twenty millions of chromatin interactions were recently identified by HiChIP at 5kb resolution (Mumbach et al. 2017). However, it has been reported that long range of chromatin interactions tends to include less CTCF at their anchors (Jeong et al. 2017). Other DNA binding proteins such as ZNF143, YY1, and SMARCA4 (BRG1) are found to be associated with chromatin interactions and EPI (Bailey et al. 2015; Barutcu et al. 2016; Weintraub et al. 2017). CTCF, cohesin, ZNF143, YY1 and SMARCA4 have other biological functions as well as chromatin interactions and EPI. The DNA binding motif sequences of the transcription factors (TF) are found in open chromatin regions near transcriptional start sites (TSS) as well as chromatin interaction anchors.

DNA binding motif sequence of ZNF143 was enriched at both chromatin interaction anchors. ZNF143's correlation with the CTCF-cohesin cluster relies on its

77 weakest binding sites, found primarily at distal regulatory elements defined by the
78 'CTCF-rich' chromatin state. The strongest ZNF143-binding sites map to promoters
79 bound by RNA polymerase II (POL2) and other promoter-associated factors, such as the
80 TATA-binding protein (TBP) and the TBP-associated protein, together forming a
81 'promoter' cluster (Bailey et al. 2015).

82 DNA binding motif sequence of YY1 does not seem to be enriched at both
83 chromatin interaction anchors (Z-score < 2), whereas DNA binding motif sequence of
84 ZNF143 is significantly enriched (Z-score > 7; Bailey et al. 2015 Figure 2a). In the
85 analysis of YY1, to identify a protein factor that might contribute to EPI, (Ji et al. 2015)
86 performed chromatin immune precipitation with mass spectrometry (ChIP-MS), using
87 antibodies directed toward histones with modifications characteristic of enhancer and
88 promoter chromatin (H3K27ac and H3K4me3, respectively). Of 26 transcription factors
89 that occupy both enhancers and promoters, four are essential based on a CRISPR
90 cell-essentiality screen and two (CTCF, YY1) are expressed in >90% of tissues
91 examined (Weintraub et al. 2017). These analyses started from the analysis of histone
92 modifications of enhancer and promoter marks rather than chromatin interactions. Other
93 protein factors associated with chromatin interactions may be found from other
94 researches.

95 As computational approaches, machine-learning analyses to predict chromatin
96 interactions have been proposed (Schreiber et al. 2017; Zhang et al. 2017). However,
97 they were not intended to find DNA motif sequences of TF affecting chromatin
98 interactions, EPI, and the expression level of transcriptional target genes, which were

99 examined in this study.

100 DNA binding proteins involved in chromatin interactions are supposed to affect
101 the transcription of genes in the loops formed by chromatin interactions. In my previous
102 analysis, the expression level of human putative transcriptional target genes was
103 affected, according to the criteria of enhancer-promoter association (EPA) (Fig. 1B;
104 (Osato 2018)). EPI were predicted based on EPA shortened at the genomic locations of
105 FR orientation of CTCF binding sites, and transcriptional target genes of each TF bound
106 in enhancers and promoters were predicted based on the EPI. The EPA affected the
107 expression levels of putative transcriptional target genes the most among three types of
108 EPAs, compared with the expression levels of transcriptional target genes predicted
109 from only promoters (Fig. 2). The expression levels tended to be increased in
110 monocytes and $CD4^+$ T cells, implying that enhancers activated the transcription of
111 genes, and decreased in ES and iPS cells, implying that enhancers repressed the
112 transcription of genes. These analyses suggested that enhancers affected the
113 transcription of genes significantly, when EPI were predicted properly. Other DNA
114 binding proteins involved in chromatin interactions, as well as CTCF, may locate at
115 chromatin interaction anchors with a pair of biased orientation of DNA binding motif
116 sequences, affecting the expression level of putative transcriptional target genes in the
117 loops formed by the chromatin interactions. As experimental issues of the analyses of
118 chromatin interactions, chromatin interaction data are changed, according to
119 experimental techniques, depth of DNA sequencing, and even replication sets of the
120 same cell type. Chromatin interaction data may not be saturated enough to cover all

121 chromatin interactions. Supposing these characters of DNA binding proteins associated
122 with chromatin interactions and avoiding experimental issues of the analyses of
123 chromatin interactions, here I searched for DNA motif sequences of TF and repeat DNA
124 sequences, affecting EPI and the expression level of putative transcriptional target genes
125 in $CD14^+$ monocytes and $CD4^+$ T cells of four people and other cell types without using
126 chromatin interaction data. Then, putative EPI were compared with chromatin
127 interaction data.
128

129 ## Results

130 **Search for biased orientation of DNA motif sequences**

131 Transcription factor binding sites (TFBS) were predicted using open chromatin
132 regions and DNA motif sequences of transcription factors (TF) collected from various
133 databases and journal papers (see Methods). Transcriptional target genes were predicted
134 using TFBS in promoters and enhancer-promoter association (EPA) shortened at the
135 genomic locations of DNA binding motif sequence of a TF acting as insulator such as
136 CTCF and cohesin (RAD21 and SMC3) (Fig. 1B). To find DNA motif sequences of TF
137 acting as insulator, other than CTCF and cohesin, and repeat DNA sequences affecting
138 the expression level of genes, EPI were predicted based on EPA shortened at the
139 genomic locations of the DNA motif sequence of a TF or a repeat DNA sequence, and
140 transcriptional target genes of each TF bound in enhancers and promoters were
141 predicted based on the EPI. The expression levels of the putative transcriptional target
142 genes were compared with those predicted from promoters using Mann Whiteney U test,

143 two-sided (p-value < 0.05) (Fig. 2A). The number of TF showing a significant
144 difference of expression level of their putative transcriptional target genes was counted.
145 To examine whether the orientation of a DNA motif sequence, which is supposed to act
146 as insulator sites and shorten EPA, affected the number of TF showing a significant
147 difference of expression level of their putative transcriptional target genes, the number
148 of the TF was compared among forward-reverse (FR), reverse-forward (RF), and any
149 orientation (i.e. without considering orientation) of a DNA motif sequence shortening
150 EPA, using chi-square test (p-value < 0.05). To avoid missing DNA motif sequences
151 showing a relatively weak statistical significance by multiple testing collection, the
152 above analyses were conducted using monocytes of four people independently, and
153 DNA motif sequences found in monocytes of four people in common were selected.
154 Total 369 of biased (232 FR and 178 RF) orientation of DNA binding motif sequences
155 of TF were found in monocytes of four people in common, whereas only seven any
156 orientation of DNA binding motif sequence was found in monocytes of four people in
157 common (Fig. 2B; Table 1; Supplemental Table S1). FR orientation of DNA motif
158 sequences included CTCF, cohesin (RAD21 and SMC3), ZNF143 and YY1, which are
159 associated with chromatin interactions and EPI. SMARCA4 (BRG1) is associated with
160 topologically associated domain (TAD), which is higher-order chromatin organization.
161 The DNA binding motif sequence of SMARCA4 was not registered in the databases
162 used in this study. FR orientation of DNA motif sequences included SMARCC2, a
163 member of the same SWI/SNF family of proteins as SMARCA4.

164 The same analysis was conducted using DNase-seq data of $CD4^+$ T cells of four

165 people. Total 376 of biased (203 FR and 213 RF) orientation of DNA binding motif
166 sequences of TF were found in T cells of four people in common, whereas only seven
167 any orientation (i.e. without considering orientation) of DNA binding motif sequences
168 were found in T cells of four people in common (Supplemental Fig. S1 and
169 Supplemental Table S2). Biased orientation of DNA motif sequences in T cells included
170 CTCF, cohesin (RAD21 and SMC3), and SMARC. Among 369, 73 of biased
171 orientation of DNA binding motif sequences of TF were found in both monocytes and T
172 cells in common (Supplemental Table S5). For each orientation, 46 FR and 34 RF
173 orientation of DNA binding motif sequences of TF were found in both monocytes and T
174 cells in common. Without considering the difference of orientation of DNA binding
175 motif sequences, 113 of biased orientation of DNA binding motif sequences of TF were
176 found in both monocytes and T cells. As a reason for the increase of the number (113)
177 from 73, a TF or an isoform of the same TF may bind to a different DNA binding motif
178 sequence according to cell types and/or in the same cell type. About 50% or more of
179 alternative splicing isoforms are differently expressed among tissues, indicating that
180 most alternative splicing is subject to tissue-specific regulation (Wang et al. 2008)
181 (Chen and Manley 2009) (Das et al. 2007). The same TF has several DNA binding
182 motif sequences and in some cases one of the motif sequences is almost the same as the
183 reverse complement sequence of another motif sequence of the same TF. For example,
184 RAD21 had both FR and RF orientation of DNA motif sequences, but the number of the
185 FR orientation of DNA motif sequence was relatively small in the genome, and the RF
186 orientation of DNA motif sequence was frequently observed and co-localized with

187 CTCF. I previously found that a complex of TF would bind to a slightly different DNA
188 binding motif sequence from the combination of DNA binding motif sequences of TF
189 composing the complex in *C. elegans* (Tabuchi et al. 2011). From another viewpoint of
190 this study, the expression level of putative transcription target genes of some TF would
191 be different, depending on the genomic locations (enhancers or promoters) of DNA
192 binding motif sequences of the TF in monocytes and T cells of four people.

193 Moreover, using open chromatin regions overlapped with H3K27ac histone
194 modification marks known as enhancer and promoter marks, the same analyses were
195 performed in monocytes and T cells. H3K27ac histone modification marks were used in
196 the analysis of EPI, but were not used in the analysis of TF as insulator like CTCF and
197 cohesin in this study, since new biased orientation of DNA motif sequences were found
198 in this criterion. When H3K27ac histone modification marks were used in the analysis
199 of TF as insulator like CTCF and cohesin, the number of biased orientation of DNA
200 motif sequences was decreased. Total 233 of biased (179 FR and 70 RF) orientation of
201 DNA binding motif sequences of TF were found in monocytes of four people in
202 common, whereas only two any orientation of DNA binding motif sequence was found
203 (Supplemental Table S3). Though the number of biased orientation of DNA motif
204 sequences was reduced, CTCF, RAD21, SMC3, ZNF143, and YY1 were found. For T
205 cells using H3K27ac histone modification marks, total 291 of biased (173 FR and 143
206 RF) orientation of DNA binding motif sequences of TF were found in T cells of four
207 people in common, whereas only 10 any orientation of DNA binding motif sequences
208 were found (Supplemental Table S4). Though the number of biased orientation of DNA

209 motif sequences was reduced, CTCF, RAD21, SMC3, and YY1 were found. Scores of
210 CTCF, RAD21, and SMC3 were increased compared with the result of T cells without
211 using H3K27ac histone modification marks, and they were ranked in the top four.
212 Biased orientation of DNA motif sequences included JUNDM2 (JDP2), which is
213 involved in histone-chaperone activity, promoting nucleosome, and inhibition of histone
214 acetylation (Jin et al. 2006). JDP2 forms a homodimer or heterodimer with various TF
215 (https://en.wikipedia.org/wiki/Jun_dimerization_protein). As summary of the results
216 with and without H3K27ac histone modification marks, total 433 of biased (306 FR and
217 178 RF) orientation of DNA motif sequences were found in monocytes of four people
218 in common. Total 499 of biased (285 FR and 278 RF) orientation of DNA motif
219 sequences were found in T cells of four people in common. Total number of these
220 results in monocytes and T cells was 773 biased (513 FR and 413 RF) orientation of
221 DNA motif sequences. Biased orientation of DNA motif sequences found in both
222 monocytes and T cells were listed in Supplemental Table S5.

223 To examine whether the biased orientation of DNA binding motif sequences of
224 TF were observed in other cell types, the same analyses were conducted in other cell
225 types. However, for other cell types, experimental data of one sample were available in
226 ENCODE database, so the analyses of DNA motif sequences were performed by
227 comparing with the result in monocytes of four people. Among the biased orientation of
228 DNA binding motif sequences found in monocytes, 61, 135, 95, and 108 DNA binding
229 motif sequences were also observed in H1-hESC, iPS, Huvec and MCF-7 respectively,
230 including CTCF and cohesin (RAD21 and SMC3) (Table 2; Supplemental Table S6).

231 The scores of DNA binding motif sequences were the highest in monocytes, and the
232 other cell types showed lower scores. The results of the analysis of DNA motif
233 sequences in $CD20^+$ B cells and macrophages did not include CTCF and cohesin,
234 because these analyses can be utilized in cells where the expression level of putative
235 transcriptional target genes of each TF show a significant difference between promoters
236 and EPA shortened at the genomic locations of a DNA motif sequence acting as
237 insulator sites. Some experimental data of a cell did not show a significant difference
238 between promoters and the EPA (Osato 2018).

239 Instead of DNA binding motif sequences of TF, repeat DNA sequences were also
240 examined. The expression levels of transcriptional target genes of each TF predicted
241 based on EPA that were shortened at the genomic locations of a repeat DNA sequence
242 were compared with those predicted from promoters. Three RF orientation of repeat
243 DNA sequences showed a significant difference of expression level of putative
244 transcriptional target genes in monocytes of four people in common (Table 3). Among
245 them, LTR16C repeat DNA sequence was observed in iPS and H1-hESC with enough
246 statistical significance considering multiple tests (p-value $< 10^{-7}$). The same as $CD14^+$
247 monocytes, biased orientation of repeat DNA sequences were examined in $CD4^+$ T cells.
248 Three FR and two RF orientation of repeat DNA sequences showed a significant
249 difference of expression level of putative transcriptional target genes in T cells of four
250 people in common (Supplemental Table S7). MIRb and MIR3 were also found in the
251 analysis using open chromatin regions overlapped with H3K27ac histone modification
252 marks, which are enhancer and promoter marks. MIR and other transposon sequences

253 are known to act as insulators and enhancers (Bejerano et al. 2006; Rebollo et al. 2012;
254 de Souza et al. 2013; Jjingo et al. 2014; Wang et al. 2015).
255
256 **Co-location of biased orientation of DNA motif sequences**
257 To examine the association of 369 biased (FR and RF) orientation of DNA
258 binding motif sequences of TF, co-location of the DNA binding motif sequences in
259 open chromatin regions was analyzed in monocytes. The number of open chromatin
260 regions with the same pairs of DNA binding motif sequences was counted, and when
261 the pairs of DNA binding motif sequences were enriched with statistical significance
262 (chi-square test, p-value $< 1.0 \times 10^{-10}$), they were listed (Table 4; Supplemental Table
263 S8). Open chromatin regions overlapped with histone modification of enhancer and
264 promoter marks (H3K27ac) (total 26,095 regions) showed a larger number of enriched
265 pairs of DNA motifs than all open chromatin regions (Table 4; Supplemental Table S8).
266 H3K27ac is known to be enriched at chromatin interaction anchors (Phanstiel et al.
267 2017). As already known, CTCF was found with cohesin such as RAD21 and SMC3
268 (Table 4). Top 30 pairs of FR and RF orientations of DNA motifs co-occupied in the
269 same open chromatin regions were shown (Table 4). Total number of pairs of DNA
270 motifs was 428, consisting of 120 unique DNA motifs, when the pair of DNA motifs
271 were observed in more than 80% of the number of open chromatin regions with the
272 DNA motifs. Biased orientation of DNA binding motif sequences of TF tended to be
273 co-localized in the same open chromatin regions.
274 To examine the association of 376 biased orientation of DNA binding motif

275 sequences of TF in $CD4^+$ T cells, co-location of the DNA binding motif sequences in
276 open chromatin regions was analyzed. Top 30 pairs of FR and RF orientations of DNA
277 motifs co-occupied in the same open chromatin regions were shown (Supplemental
278 Table S9). Total number of pairs of DNA motifs was 99, consisting of 72 unique DNA
279 motifs, when the pair of DNA motifs were observed in more than 80% of the number of
280 open chromatin regions with the DNA motifs (chi-square test, p-value $< 1.0 \times 10^{-10}$).
281 Among them, 11 pairs of DNA motif sequences including a pair of CTCF, SMC3, and
282 RAD21 in T cells were found in monocytes in common (Supplemental Table S9).
283
284 **Comparison with chromatin interaction data**
285 To examine whether the biased orientation of DNA motif sequences is associated
286 with chromatin interactions, enhancer-promoter interactions (EPI) predicted based on
287 enhancer-promoter associations (EPA) were compared with chromatin interaction data
288 (Hi-C). Due to the resolution of Hi-C experimental data used in this study (50kb), EPI
289 were adjusted to 50kb resolution. EPI were predicted based on three types of EPA: (i)
290 EPA shortened at the genomic locations of FR or RF orientation of DNA motif
291 sequence of a TF, (ii) EPA shortened at the genomic locations of DNA motif sequence
292 of a TF acting as insulator sites such as CTCF and cohesin (RAD21, SMC3) without
293 considering their orientation, and (iii) EPA without being shortened by the genomic
294 locations of a DNA motif sequence. EPA (i) showed a significantly higher ratio of EPI
295 overlapped with chromatin interactions (Hi-C) using DNA binding motif sequences of
296 CTCF and cohesin (RAD21 and SMC3) than the other two types of EPAs (n = 4,

297 binomial test, two-sided) (Supplemental Fig. S2). Total 58 biased orientation (38 FR
298 and 22 RF) of DNA motif sequences including CTCF, cohesin, and YY1 showed a
299 significantly higher ratio of EPI overlapped with Hi-C chromatin interactions (a cutoff
300 score of CHiCAGO tool > 1) than the other types of EPAs in monocytes (Supplemental
301 Table S10). When comparing EPI predicted based on only EPA (i) and (iii) with
302 chromatin interactions, total 215 biased orientation (130 FR and 102 RF) of DNA motif
303 sequences showed a significantly higher ratio of EPI predicted based on EPA (i)
304 overlapped with the chromatin interactions than EPI predicted based on EPA (iii)
305 (Supplemental material 2). The difference between EPI predicted based on EPA (i) and
306 (ii) seemed to be difficult to distinguish using the chromatin interaction data and the
307 statistical test in some cases. However, as for the difference between EPI predicted
308 based on EPA (i) and (iii), a larger number of biased orientation of DNA motif
309 sequences was found to be correlated with chromatin interaction data. Chromatin
310 interaction data were obtained from different samples from DNase-seq, open chromatin
311 regions, so individual differences seemed to be large from the results of this analysis.
312 Since, for some DNA motif sequences of transcription factors, the number of EPI
313 overlapped with chromatin interactions was small, if higher resolution of chromatin
314 interaction data (such as HiChIP, in situ DNase Hi-C, and in situ Hi-C data, or a tool to
315 improve the resolution such as HiCPlus) is available, the number of EPI overlapped
316 with chromatin interactions would be increased and the difference of the numbers
317 among three types of EPA would be larger and more significant (Rao et al. 2014;
318 Ramani et al. 2016; Mumbach et al. 2017; Zhang et al. 2018).

319 After the analysis of $CD14^+$ monocytes, to utilize HiChIP chromatin interaction
320 data in $CD4^+$ T cells, the same analysis for $CD14^+$ monocytes was performed using
321 DNase-seq data of four donors in $CD4^+$ T cells (Mumbach et al. 2017). EPI predicted
322 based on EPA were compared with three replications (B2T1, B2T2, and B3T1) of
323 HiChIP chromatin interaction data in $CD4^+$ T cells respectively. The resolutions of
324 HiChIP chromatin interaction data and EPI were adjusted to 5kb. EPI were predicted
325 based on the three types of EPA in the same way as $CD14^+$ monocytes using top 60%
326 expression level of all transcripts (genes) excluding transcripts not expressed in T cells.
327 The criteria of the analysis were determined to include known DNA motif sequences
328 involved in chromatin interactions such as CTCF and cohesin in the result, and the
329 result was consistent with that using Hi-C chromatin interaction data. EPA (iii) showed
330 the highest ratio of EPI overlapped with chromatin interactions (HiChIP) using DNA
331 binding motif sequences of CTCF and cohesin (RAD21 and SMC3), compared with the
332 other two types of EPA (i) and (ii) (n = 4, binomial test, two-sided, 95% confidence
333 interval) (Fig. 3). Total 136 biased orientation (70 FR and 73 RF) of DNA motif
334 sequences, which included CTCF, cohesin (RAD21 and SMC3), and SMARC in three
335 replications (B2T1, B2T2, and B3T1) and ZNF143 in two replications (B2T2 and
336 B3T1), showed a significantly higher ratio of EPI overlapped with HiChIP chromatin
337 interactions (more than 1,000 counts for each interaction) than the other types of EPAs
338 in T cells (Table 5). When comparing EPI predicted based on only EPA (i) and (iii) with
339 the chromatin interactions, total 356 biased orientation (194 FR and 200 RF) of DNA
340 motif sequences showed a significantly higher ratio of EPI predicted based on EPA (iii)

341 overlapped with the chromatin interactions than EPI predicted based on EPA (i) (Table
342 5; Supplemental material 2). As expected, the number of EPI overlapped with
343 chromatin interactions (HiChIP) was increased, compared with Hi-C chromatin
344 interactions. Most of biased orientation of DNA motif sequences (95%) were found to
345 be correlated with chromatin interactions, when comparing EPI predicted based on EPA
346 (i) and (iii) with HiChIP chromatin interactions.

347 Moreover, to examine the enhancer activity of EPI, the distribution of expression
348 level of putative target genes of EPI was compared between EPI overlapped with
349 HiChIP chromatin interactions and EPI not overlapped with them. Though the target
350 genes of EPI were selected from top 60% expression level of all transcripts (genes)
351 excluding transcripts not expressed in T cells, target genes of EPI overlapped with
352 chromatin interactions showed a significantly higher expression level than EPI not
353 overlapped with them, suggesting that EPI overlapped with chromatin interactions
354 activated the expression of target genes in T cells. Almost all (99.9%) FR and RF
355 orientations of DNA motifs showed a significantly higher expression level of putative
356 target genes of EPI overlapped with chromatin interactions than EPI not overlapped.
357 When a biased orientation of DNA motif showed a significantly higher expression level
358 of putative target genes of EPI overlapped with chromatin interactions than EPI not
359 overlapped, '1' was marked with in the tables of the comparison between EPI and
360 HiChIP chromatin interactions in Supplemental material 2. When a DNA motif showed
361 a significantly lower expression level, '-1' was marked with, however, it was not
362 observed in this analysis. When there was not significant difference of expression level,

363 ‘0’ was marked with.

364 If biased orientation of DNA motif sequences of TF found in both monocytes and
365 T cells are biologically meaningful, these may match the result of the analysis of
366 HiChIP data. Among 376 FR and RF orientations of biased orientation of DNA motifs
367 of TF in T cells, 136 (36%) were biased orientation of DNA motifs in the analysis of
368 HiChIP data for three types of EPA (i) (ii) and (iii). Among 73 FR and RF orientations
369 of DNA motifs of TF found in both monocytes and T cells, 31 (42%) were biased
370 orientation of DNA motifs in the analysis of HiChIP data, which was significantly
371 higher ratio than all 376 biased orientation of DNA motifs in T cell, and included CTCF,
372 RAD21 and SMC3 (p-value < 0.015, binomial test, two-sided, 95% confidence interval)
373 (Supplemental Table S5 and Table 5). However, this may not imply that all 376 biased
374 orientation of DNA motifs included false-positive predictions, and may be due to the
375 limitation of resolution of the HiChIP data (5kb) or the small number of DNA binding
376 sites of a TF in genome sequences. Then, among 113 FR and RF orientations of DNA
377 motifs of TF found in both monocytes and T cells without considering the difference of
378 orientation (FR or RF) of DNA binding motifs, 42 (37%) were biased orientation of
379 DNA motifs in the analysis of HiChIP data, which was not significantly higher ratio.
380 This implied that the difference of orientation of DNA motifs was important to predict
381 EPI in comparison with HiChIP data.

382 Though the ratios of EPI overlapped with chromatin interactions were increased
383 by using many chromatin interaction data including lower score and count of chromatin
384 interactions (a cutoff score of CHiCAGO tool > 1 for Hi-C and more than 1,000 counts

385 for HiChIP), the ratios of EPI overlapped with chromatin interactions showed the same
386 tendency among the three types of EPAs. The ratio of EPI overlapped with Hi-C
387 chromatin interactions was increased using H3K27ac marks in both monocytes and T
388 cells. The ratio of EPI overlapped with HiChIP chromatin interactions was also
389 increased using H3K27ac marks. Chromatin interaction data were obtained from
390 different samples from DNase-seq, open chromatin regions in $CD4^+$ T cells, so
391 individual differences seemed to be large from the results of this analysis, and
392 (Mumbach et al. 2017) suggested that individual differences of chromatin interactions
393 were larger than those of open chromatin regions. ATAC-seq data, open chromatin
394 regions were available in $CD4^+$ T cells in the paper, however, when using ATAC-seq
395 data, the result of the analysis of biased orientation of DNA motif sequences was
396 different from DNase-seq data, and not included a part of CTCF and cohesin. Thus,
397 DNase-seq data collected from ENCODE and Blueprint projects were employed in this
398 study.
399

400 **Discussion**

401 To find DNA motif sequences of transcription factors (TF) and repeat DNA
402 sequences affecting the expression level of human putative transcriptional target genes,
403 the DNA motif sequences were searched from open chromatin regions of monocytes of
404 four people. Total 369 biased [232 forward-reverse (FR) and 178 reverse-forward (RF)]
405 orientation of DNA motif sequences of TF were found in monocytes of four people in
406 common, whereas only seven any orientation (i.e. without considering orientation) of

407 DNA motif sequence of TF was found to affect the expression level of putative
408 transcriptional target genes, suggesting that enhancer-promoter association (EPA)
409 shortened at the genomic locations of FR or RF orientation of the DNA motif sequence
410 of a TF or a repeat DNA sequence is an important character for the prediction of
411 enhancer-promoter interactions (EPI) and the transcriptional regulation of genes.

412 When DNA motif sequences were searched from monocytes of one person, a
413 larger number of biased orientation of DNA motif sequences affecting the expression
414 level of human putative transcriptional target genes were found. When the number of
415 donors, from which experimental data were obtained, was increased, the number of
416 DNA motif sequences found in all people in common decreased and in some cases,
417 known transcription factors involved in chromatin interactions such as CTCF and
418 cohesin (RAD21 and SMC3) were not identified by statistical tests. This would be
419 caused by individual difference of the same cell type, low quality of experimental data,
420 and experimental errors. Moreover, though FR orientation of DNA binding motif
421 sequences of CTCF and cohesin is frequently observed at chromatin interaction anchors,
422 the percentage of FR orientation is not 100, and other orientations of the DNA binding
423 motif sequences are also observed. Though DNA binding motif sequences of CTCF and
424 cohesin are found in various open chromatin regions, DNA binding motif sequences of
425 some TF would be observed less frequently in open chromatin regions. The analyses of
426 experimental data of a number of people would avoid missing relatively weak statistical
427 significance of DNA motif sequences of TF in experimental data of each person by
428 multiple testing correction of thousands of statistical tests. A DNA motif sequence was

429 found with p-value < 0.05 in experimental data of one person and the DNA motif
430 sequence found in the same cell type of four people in common would have p-value <
431 $0.05^4 = 6.25 \times 10^{-6}$. Actually, DNA motif sequences with p-value slightly less than
432 0.05 in monocytes of one person were observed in monocytes of four people in
433 common.

434 EPI were compared with chromatin interactions (Hi-C) in monocytes. EPAs
435 shortened at the genomic locations of DNA binding motif sequences of CTCF and
436 cohesin (RAD21 and SMC3) showed a significant difference of the ratios of EPI
437 overlapped with chromatin interactions, according to three types of EPAs (see Methods).
438 Using open chromatin regions overlapped with ChIP-seq experimental data of histone
439 modification of an enhancer mark (H3K27ac), the ratio of EPI not overlapped with
440 Hi-C was reduced. (Phanstiel et al. 2017) also reported that there was an especially
441 strong enrichment for loops with H3K27 acetylation peaks at both ends (Fisher's Exact
442 Test, $p = 1.4 \times 10^{-27}$). However, the total number of EPI overlapped with chromatin
443 interactions was also reduced using H3K27ac peaks, so more chromatin interaction data
444 would be needed to obtain reliable results in this analysis. As an issue of experimental
445 data, data for chromatin interactions and open chromatin regions were came from
446 different samples and donors, so individual differences would exist in the data.
447 Moreover, the resolution of chromatin interaction data used in monocytes was about
448 50kb, thus the number of chromatin interactions was relatively small (72,284 at 50kb
449 resolution with a cutoff score of CHiCAGO tool > 1 and 16,501 with a cutoff score of
450 CHiCAGO tool > 5). EPI predicted based on EPA shortened at the genomic locations of

451 DNA binding motif sequence of TF that were found in various open chromatin regions
452 such as CTCF and cohesin (RAD21 and SMC3) tended to be overlapped with a larger
453 number of chromatin interactions than TF less frequently observed in open chromatin
454 regions. Therefore, to examine the difference of the numbers of EPI overlapped with
455 chromatin interactions, according to the three types of EPAs, the number of chromatin
456 interactions should be large enough.

457 As HiChIP chromatin interaction data were available in $CD4^+$ T cells, biased
458 orientation of DNA motif sequences of TF were examined in T cells using DNase-seq
459 data of four people. The resolutions of chromatin interactions and EPI were adjusted to
460 5kb by fragmentation of genome sequences. In monocytes, the resolution of Hi-C
461 chromatin interaction data was converted by extending anchor regions of chromatin
462 interactions to 50kb length and merging the chromatin interactions overlapped with
463 each other. Fragmentation of genome sequences may affect the classification of
464 chromatin interactions of which anchors are located near the border of a fragment, but
465 the number of chromatin interactions would not be decreased, compared with merging
466 chromatin interactions. The number of HiChIP chromatin interactions was 19,926,360
467 at 5kb resolution, 666,149 at 5kb resolution with chromatin interactions (more than
468 1,000 counts for each interaction), and 78,209 at 5kb resolution with chromatin
469 interactions (more than 6,000 counts for each interaction). As expected, the number of
470 EPI overlapped with chromatin interactions was increased, and 36 – 95% of biased
471 orientation of DNA motif sequences of TF showed a statistical significance in EPI
472 predicted based on EPA shortened at the genomic locations of the DNA motif sequence,

473 compared with the other types of EPAs or EPA not shortened. False positive predictions
474 of EPI would be decreased by using H3K27ac marks and other features. The ratio of
475 EPI overlapped with Hi-C chromatin interactions was increased using H3K27ac marks
476 in both monocytes and T cells. The ratio of EPI overlapped with HiChIP chromatin
477 interactions was also increased using H3K27ac marks. However, the number of biased
478 orientation of DNA motif sequences showing a higher ratio of EPI overlapped with
479 HiChIP chromatin interactions than the other types of EPAs was decreased using
480 H3K27ac marks (Supplemental material 2).

481 When forming a homodimer or heterodimer with another TF, TF may bind to
482 genome DNA with a specific orientation of their DNA binding sequences (Fig. 4). From
483 the analysis of biased orientation of DNA motif sequences of TF, TF forming
484 heterodimer would also be found. If the DNA binding motif sequence of only the mate
485 to a pair of TF was found in EPA, EPA was shortened at one side, which is the genomic
486 location of the DNA binding motif sequence of the mate to the pair, and transcriptional
487 target genes were predicted using the EPA shortened at the side. In this analysis, the
488 mate to both heterodimer and homodimer of TF can be used to examine the effect on
489 the expression level of transcriptional target genes predicted based on the EPA
490 shortened at one side. For heterodimer, biased orientation of DNA motif sequences may
491 also be found in forward-forward or reverse-reverse orientation.

492 Some DNA binding sites of TF predicted using DNA binding motif sequences of
493 TF were changed according to the parameters of FIMO tool, particularly background
494 frequencies of ATGC nucleotides in genome sequences and *p*-value threshold. Repeat

495 DNA sequences also affected the result of the prediction. Without repeat masking, the
496 number of any orientation of DNA motifs of TF was increased. However, the *p*-value of
497 the DNA motifs was relatively high and close to the threshold, so these DNA motifs
498 seemed to be false positives. To decrease false-positive and false-negative predictions
499 of DNA binding sites of TF, improve the prediction of biased orientation of DNA
500 motifs, and obtain a robust result of the analysis, there may be a room to explore more
501 suitable parameters and methods, such as stricter *p*-value threshold, using genomic
502 regions conserved among species, masking some exons encoding mRNA, removing
503 DNA motifs highly affected by parameter changes (low information content), changing
504 the parameter of nucleotide frequencies according to genomic regions, considering
505 epigenetic modifications (DNA methylation and histone) and so on. For the analysis of
506 EPI, instead of using all DNA motif sequences of TF in databases, selecting DNA motif
507 sequences of TF indicating enhancer activity in a cell type using my method would
508 reduce the effect of TF not acting as enhancer (Osato 2018).

509 It has been reported that CTCF and cohesin-binding sites are frequently mutated
510 in cancer (Katainen et al. 2015). Some biased orientation of DNA motif sequences
511 would be associated with chromatin interactions and might be associated with diseases
512 including cancer.

513 The analyses in this study revealed novel characters of DNA binding motif
514 sequences of TF and repeat DNA sequences to analyze TF involved in chromatin
515 interactions, insulator function and forming a homodimer, heterodimer or complex with
516 other TF, affecting the transcriptional regulation of genes.

517

518 ## Methods

519 **Search for biased orientation of DNA motif sequences**

520 To examine transcriptional regulatory target genes of transcription factors (TF),
521 bed files of hg38 of Blueprint DNase-seq data for $CD14^+$ monocytes of four donors
522 (EGAD00001002286; Donor ID: C0010K, C0011I, C001UY, C005PS) were obtained
523 from Blueprint project web site (http://dcc.blueprint-epigenome.eu/#/home), and the bed
524 files of hg38 were converted into those of hg19 using Batch Coordinate Conversion
525 (liftOver) web site (https://genome.ucsc.edu/util.html). Bed files of hg19 of ENCODE
526 H1-hESC (GSM816632; UCSC Accession: wgEncodeEH000556), iPSC (GSM816642;
527 UCSC Accession: wgEncodeEH001110), HUVEC (GSM1014528; UCSC Accession:
528 wgEncodeEH002460), and MCF-7 (GSM816627; UCSC Accession:
529 wgEncodeEH000579) were obtained from the ENCODE websites
530 (http://hgdownload.cse.ucsc.edu/goldenPath/hg19/encodeDCC/wgEncodeUwDgf/;
531 http://hgdownload.cse.ucsc.edu/goldenPath/hg19/encodeDCC/wgEncodeUwDnase/).

532 As high resolution of chromatin interaction data using HiChIP became available
533 in $CD4^+$ T cells, to promote the same analysis of $CD14^+$ monocytes in $CD4^+$ T cells,
534 DNase-seq data of four donors were obtained from a public database and Blueprint
535 projects web sites. DNase-seq data of only one donor was available in Blueprint project
536 for $CD4^+$ T cells (Donor ID: S008H1), and three other DNase-seq data were obtained
537 from NCBI Gene Expression Omnibus (GEO) database. Though the peak calling of
538 DNase-seq data available in GEO database was different from other DNase-seq data in

539 ENCODE and Blueprint projects where 150bp length of peaks were usually predicted
540 using HotSpot (John et al. 2011), FASTQ files of DNase-seq data were downloaded
541 from NCBI Sequence Read Archive (SRA) database (SRR097566, SRR097618, and
542 SRR171574). Read sequences of the FASTQ files were aligned to the hg19 version of
543 the human genome reference using BWA (Li and Durbin 2009), and the BAM files
544 generated by BWA were converted into SAM files, sorted, and indexed using Samtools
545 (Li et al. 2009). Peaks of the DNase-seq data were predicted using HotSpot-4.1.1.

546 To identify transcription factor binding sites (TFBS) from the DNase-seq data,
547 TRANSFAC (2019.1), JASPAR (2018), UniPROBE (2018), BEEML-PBM,
548 high-throughput SELEX, Human Protein-DNA Interactome, transcription factor
549 binding sequences of ENCODE ChIP-seq data, and HOCOMOCO version 9 and 11
550 were used to predict insulator sites (Wingender et al. 1996; Newburger and Bulyk 2009;
551 Portales-Casamar et al. 2010; Xie et al. 2010; Zhao and Stormo 2011; Jolma et al. 2013;
552 Kheradpour and Kellis 2014) (Kulakovskiy et al. 2018). TRANSFAC (2011.1),
553 JASPAR (2012), UniPROBE (2012), BEEML-PBM, high-throughput SELEX, and
554 Human Protein-DNA Interactome were used to analyze enhancer-promoter interactions,
555 since these data were sufficient to identify biased orientation of DNA motif sequences
556 of TF with less computational time, reducing the number of any orientation of DNA
557 motif sequences of TF. Position weight matrices of transcription factor binding
558 sequences were transformed into TRANSFAC matrices and then into MEME matrices
559 using in-house scripts and transfac2meme in MEME suite (Bailey et al. 2009).
560 Transcription factor binding sequences of TF derived from vertebrates were used for

561 further analyses. Transcription factor binding sequences were searched from each
562 narrow peak of DNase-seq data in repeat-masked hg19 genome sequences using FIMO
563 with *p*-value threshold of 10^{-5} and background frequencies of ATGC nucleotides in
564 repeat-masked hg19 genome sequences (Grant et al. 2011). Repeat-masked hg19
565 genome sequences were downloaded from UCSC genome browser
566 (http://genome.ucsc.edu/,
567 http://hgdownload.soe.ucsc.edu/goldenPath/hg19/bigZips/hg19.fa.masked.gz). TF
568 corresponding to transcription factor binding sequences were searched computationally
569 by comparing their names and gene symbols of HGNC (HUGO Gene Nomenclature
570 Committee) -approved gene nomenclature and 31,848 UCSC known canonical
571 transcripts
572 (http://hgdownload.soe.ucsc.edu/goldenPath/hg19/database/knownCanonical.txt.gz), as
573 transcription factor binding sequences were not linked to transcript IDs such as UCSC,
574 RefSeq, and Ensembl transcripts.
575 Target genes of a TF were assigned when its TFBS was found in DNase-seq
576 narrow peaks in promoter or extended regions for enhancer-promoter association of
577 genes (EPA). Promoter and extended regions were defined as follows: promoter regions
578 were those that were within distance of ±5 kb from transcriptional start sites (TSS).
579 Promoter and extended regions were defined as per the following association rule,
580 which is the same as that defined in Figure 3A of a previous study (McLean et al.
581 2010): the single nearest gene association rule, which extends the regulatory domain to
582 the midpoint between the TSS of the gene and that of the nearest gene upstream and

583 downstream without the limitation of extension length. Extended regions for EPA were
584 shortened at the genomic locations of DNA binding sites of a TF that was the closest to
585 a transcriptional start site, and transcriptional target genes were predicted from the
586 shortened enhancer regions using TFBS. Furthermore, promoter and extended regions
587 for EPA were shortened at the genomic locations of forward–reverse (FR) orientation of
588 DNA binding sites of a TF. When forward or reverse orientation of DNA binding sites
589 were continuously located in genome sequences several times, the most external
590 forward–reverse orientation of DNA binding sites were selected. The genomic positions
591 of genes were identified using 'knownGene.txt.gz' file in UCSC bioinformatics sites
592 (Karolchik et al. 2014). The file 'knownCanonical.txt.gz' was also utilized for choosing
593 representative transcripts among various alternate forms for assigning promoter and
594 extended regions for EPA. From the list of transcription factor binding sequences and
595 transcriptional target genes, redundant transcription factor binding sequences were
596 removed by comparing the target genes of a transcription factor binding sequence and
597 its corresponding TF; if identical, one of the transcription factor binding sequences was
598 used. When the number of transcriptional target genes predicted from a transcription
599 factor binding sequence was less than five, the transcription factor binding sequence
600 was omitted.

601 Repeat DNA sequences were searched from the hg19 version of the human
602 reference genome using RepeatMasker (Smit, AFA & Green, P RepeatMasker at
603 http://www.repeatmasker.org) and RepBase RepeatMasker Edition
604 (http://www.girinst.org).

605 For gene expression data, RNA-seq reads mapped onto human hg19 genome
606 sequences were obtained, including ENCODE long RNA-seq reads with poly-A of
607 H1-hESC, iPSC, HUVEC, and MCF-7 (GSM26284, GSM958733, GSM2344099,
608 GSM2344100, GSM958734, and GSM765388), and UCSF-UBC human reference
609 epigenome mapping project RNA-seq reads with poly-A of naive $CD4^+$ T cells
610 (GSM669617). Two replicates were present for H1-hESC, iPSC, HUVEC, and MCF-7,
611 and a single one for $CD4^+$ T cells. FPKMs of the RNA-seq data were calculated using
612 RSeQC (Wang et al. 2012). For monocytes, Blueprint RNA-seq FPKM data
613 ('C0010KB1.transcript_quantification.rsem_grape2_crg.GRCh38.20150622.results',
614 'C0011IB1.transcript_quantification.rsem_grape2_crg.GRCh38.20150622.results',
615 'C001UYB4.transcript_quantification.rsem_grape2_crg.GRCh38.20150622.results',
616 and 'C005PS12.transcript_quantification.rsem_grape2_crg.GRCh38.20150622.results')
617 were downloaded from Blueprint DCC portal
618 (http://dcc.blueprint-epigenome.eu/#/files). Based on FPKM, UCSC transcripts with top
619 50% expression level of all the transcripts excluding transcripts not expressed were
620 selected in each cell type.
621 The expression level of transcriptional target genes predicted based on EPA
622 shortened at the genomic locations of DNA motif sequence of a TF or a repeat DNA
623 sequence was compared with the expression level of transcriptional target genes
624 predicted from promoter. For each DNA motif sequence shortening EPA,
625 transcriptional target genes were predicted using about 3,000 – 5,000 DNA binding
626 motif sequences of TF, and the distribution of expression level of putative

627 transcriptional target genes of each TF was compared between EPA and only promoter
628 using Mann-Whitney test, two-sided (p-value < 0.05). The number of TF showing a
629 significant difference of expression level of putative transcriptional target genes
630 between EPA and promoter was compared among forward-reverse (FR),
631 reverse-forward (RF), and any orientation (i.e. without considering orientation) of a
632 DNA motif sequence shortening EPA using chi-square test (p-value < 0.05). When a
633 DNA motif sequence of a TF or a repeat DNA sequence shortening EPA showed a
634 significant difference of expression level of putative transcriptional target genes among
635 FR, RF, or any orientation in monocytes of four people in common, the DNA motif
636 sequence was listed.

637 Though forward-reverse orientation of DNA binding motif sequences of CTCF
638 and cohesin are frequently observed at chromatin interaction anchors, the percentage of
639 forward-reverse orientation is not 100, and other orientations of the DNA binding motif
640 sequences are also observed. Though DNA binding motif sequences of CTCF and
641 cohesin are found in various open chromatin regions, DNA binding motif sequences of
642 some transcription factors would be observed less frequently in open chromatin regions.
643 The analyses of experimental data of a number of people would avoid missing relatively
644 weak statistical significance of DNA motif sequences in experimental data of each
645 person by multiple testing correction of thousands of statistical tests. A DNA motif
646 sequence was found with p-value < 0.05 in experimental data of one person and the
647 DNA motif sequence found in the same cell type of four people in common would have
648 p-value $< 0.05^4 = 6.25 \times 10^{-6}$.

649

650 **Co-location of biased orientation of DNA motif sequences**

651 Co-location of biased orientation of DNA binding motif sequences of TF was
652 examined. The number of open chromatin regions with the same pair of DNA binding
653 motif sequences was counted, and when the pair of DNA binding motif sequences were
654 enriched with statistical significance (chi-square test, *p*-value $< 1.0 \times 10^{-10}$), they were
655 listed. For histone modification of an enhancer mark (H3K27ac), bed files of hg38 of
656 Blueprint ChIP-seq data for $CD14^+$ monocytes (EGAD00001001179) and $CD4^+$ T cells
657 (Donor ID: S000RD) were obtained from Blueprint web site
658 (http://dcc.blueprint-epigenome.eu/#/home), and the bed files of hg38 were converted
659 into those of hg19 using Batch Coordinate Conversion (liftOver) web site
660 (https://genome.ucsc.edu/util.html). Networks of co-locations of biased orientation of
661 DNA motif sequences were plotted using Cytoscape v3.71 with yFiles Layout
662 Algorithms for Cytoscape (Shannon et al. 2003).

663

664 **Comparison with chromatin interaction data**

665 For comparison of EPA in monocytes with chromatin interactions,
666 'PCHiC_peak_matrix_cutoff0.txt.gz' file was downloaded from 'Promoter Capture
667 Hi-C in 17 human primary blood cell types' web site (https://osf.io/u8tzp/files/), and
668 chromatin interactions for Monocytes with scores of CHiCAGO tool > 1 and
669 CHiCAGO tool > 5 were extracted from the file (Javierre et al. 2016). In the same way
670 as monocytes, Hi-C chromatin interaction data of $CD4^+$ T cells (Naive $CD4^+$ T cells,

671 nCD4) were obtained.

672 Enhancer-promoter interactions (EPI) were predicted using three types of EPAs
673 in monocytes: (i) EPA shortened at the genomic locations of FR or RF orientation of
674 DNA motif sequence of a TF, (ii) EPA shortened at the genomic locations of any
675 orientation (i.e. without considering orientation) of DNA motif sequence of a TF, and
676 (iii) EPA without being shortened by a DNA motif sequence. EPI predicted using the
677 three types of EPAs in common were removed. First, EPI predicted based on EPA (i)
678 were compared with chromatin interactions (Hi-C). The resolution of chromatin
679 interaction data used in this study was 50kb, so EPI were adjusted to 50kb before their
680 comparison. The number and ratio of EPI overlapped with chromatin interactions were
681 counted. Second, EPI were predicted based on EPA (ii), and EPI predicted based on
682 EPA (i) were removed from the EPI. The number and ratio of EPI overlapped with
683 chromatin interactions were counted. Third, EPI were predicted based on EPA (iii), and
684 EPI predicted based on EPA (i) and (ii) were removed from the EPI. The number and
685 ratio of EPI overlapped with chromatin interactions were counted. The number and ratio
686 of the EPI were compared two times between EPA (i) and (iii), and EPA (i) and (ii)
687 (binomial distribution, p-value < 0.025 for each test, two-sided, 95% confidence
688 interval).

689 For comparison of EPA with chromatin interactions (HiChIP) in $CD4^+$ T cells,
690 'GSM2705049_Naive_HiChIP_H3K27ac_B2T1_allValidPairs.txt',
691 'GSM2705050_Naive_HiChIP_H3K27ac_B2T2_allValidPairs.txt', and
692 'GSM2705051_Naive_HiChIP_H3K27ac_B3T1_allValidPairs.txt' files were

693 downloaded from Gene Expression Omnibus (GEO) database (GSM2705049,
694 GSM2705050 and GSM2705051). The resolutions of chromatin interaction data and
695 EPI were adjusted to 5kb before their comparison. Chromatin interactions with more
696 than 6,000 and 1,000 counts for each interaction were used in this study.

697 Putative target genes for the analysis of EPI were selected from top 50%
698 expression level of all transcripts excluding transcripts not expressed in monocytes and
699 top 60% expression level of transcripts in $CD4^+$ T cells. The expression level of putative
700 target genes of EPI overlapped with HiChIP chromatin interactions was compared with
701 EPI not overlapped with them. For each FR or RF orientation of DNA motif, EPI were
702 predicted based on EPA and the overlap of EPI with chromatin interactions was
703 examined. When a putative transcriptional target gene of a TF in an enhancer was found
704 in both EPI overlapped with a chromatin interaction and EPI not overlapped with, the
705 target gene was removed. The distribution of expression level of putative target genes
706 was compared using Mann-Whitney test, two-sided (p-value < 0.05).

707

708 **Acknowledgements**

709 The supercomputing resource was provided by Human Genome Center of the Institute
710 of Medical Science at the University of Tokyo. Computations were partially performed
711 on the NIG supercomputer at ROIS National Institute of Genetics. Publication charges
712 for this article were funded by JSPS KAKENHI Grant Number 16K00387. This
713 research was partially supported by the Platform Project for Supporting in Drug
714 Discovery and Life Science Research（Platform for Dynamic Approaches to Living

715 System）from Japan Agency for Medical Research and Development (AMED). This
716 research was partially supported by Development of Fundamental Technologies for
717 Diagnosis and Therapy Based upon Epigenome Analysis from Japan Agency for
718 Medical Research and Development (AMED). This work was partially supported by
719 JST CREST Grant Number JPMJCR15G1, Japan.
720

721 **Figures**

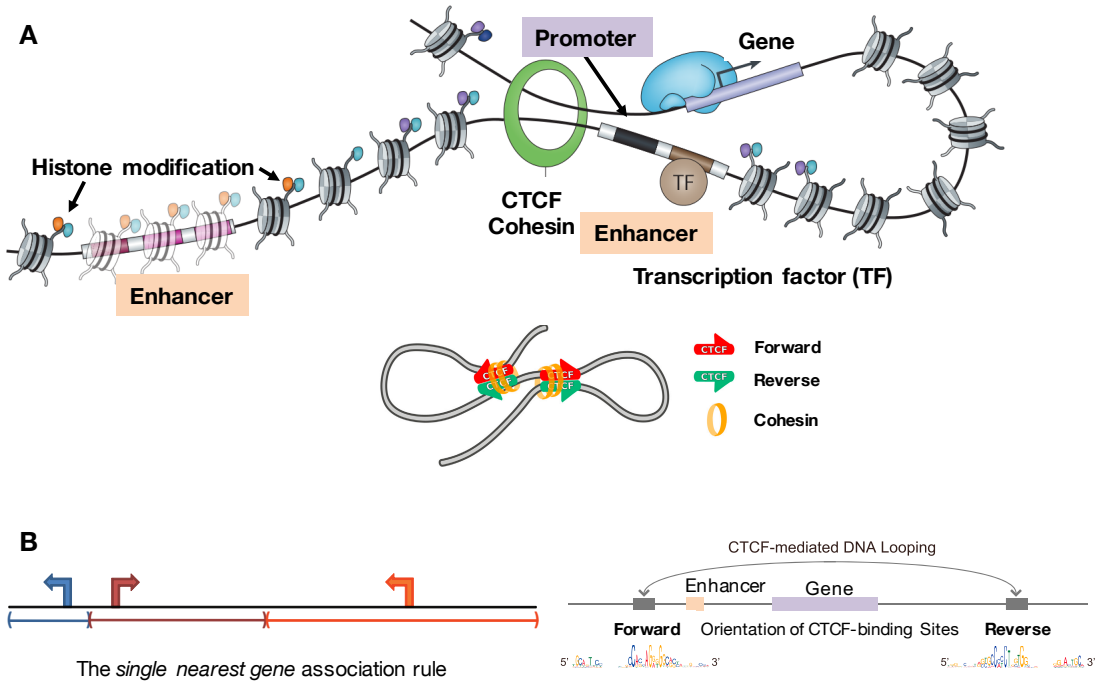

722

723 **Figure 1.** Chromatin interactions and enhancer-promoter association. (A) Forward–
724 reverse orientation of CTCF-binding sites are frequently found in chromatin interaction
725 anchors. CTCF can block the interaction between enhancers and promoters limiting the
726 activity of enhancers to certain functional domains (de Wit et al. 2015; Guo et al. 2015).
727 (B) Computationally-defined regulatory domains for enhancer-promoter association
728 (McLean et al. 2010). The *single nearest gene* association rule extends the regulatory
729 domain to the midpoint between this gene's TSS and the nearest gene's TSS both
730 upstream and downstream. Enhancer-promoter association was shortened at the
731 genomic locations of forward-reverse orientation of DNA binding motif sequence of a
732 transcription factor (e.g. CTCF in the figure).

733

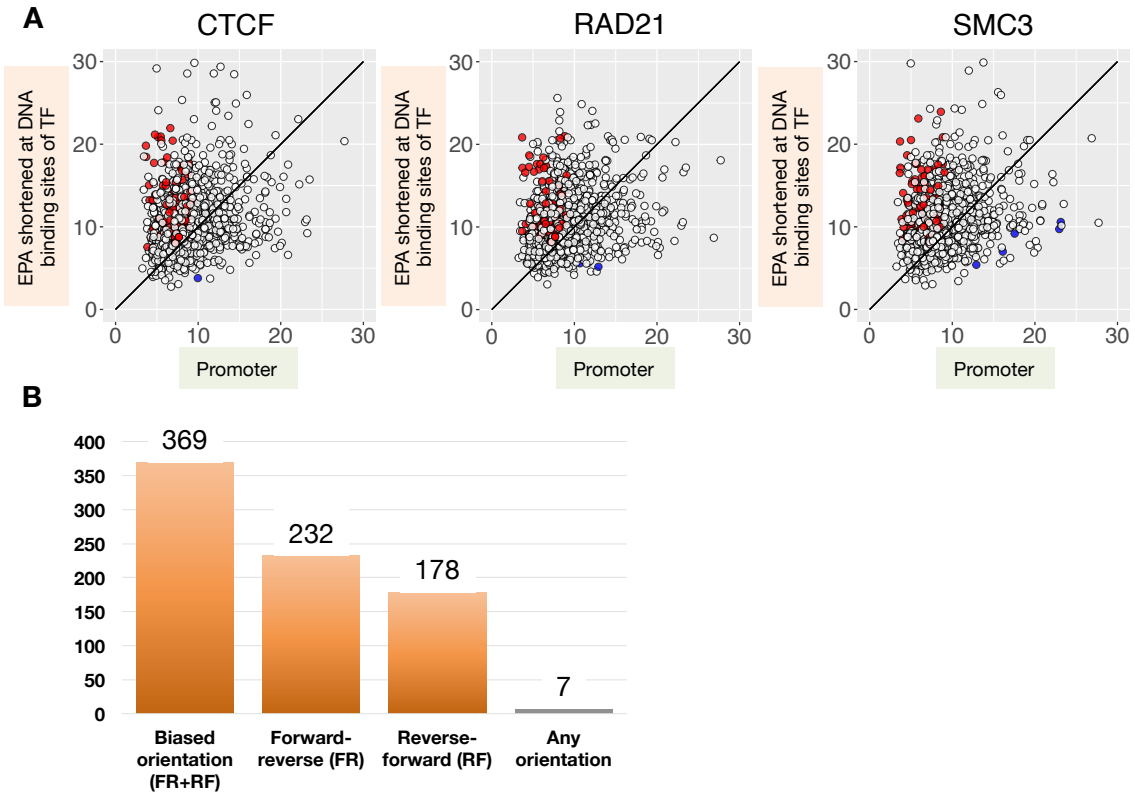

Figure 2. Biased orientation of DNA motif sequences of transcription factors affecting the transcription of genes. (A) Comparison of expression level of putative transcriptional target genes. The median expression levels of target genes of the same transcription factor binding sequences were compared between promoters and enhancer-promoter association (EPA) shortened at the genomic locations of forward-reverse orientation of DNA motif sequence of CTCF and cohesin (RAD21 and SMC3) respectively in monocytes. Red and blue dots show statistically significant difference (Mann-Whitney test) of the distribution of expression levels of target genes between promoters and the EPA. Red dots show the median expression level of target genes was higher based on the EPA than promoters, and blue dots show the median expression level of target genes was lower based on the EPA than promoters. The

746 expression level of target genes predicted based on the EPA tended to be higher than
747 promoters, implying that transcription factors acted as activators of target genes. (B)
748 Biased orientation of DNA motif sequences of transcription factors in monocytes. Total
749 369 of biased orientation of DNA binding motif sequences of transcription factors were
750 found to affect the expression level of putative transcriptional target genes in monocytes
751 of four people in common, whereas only one any orientation (i.e. without considering
752 orientation) of DNA binding motif sequence was found to affect the expression level.
753

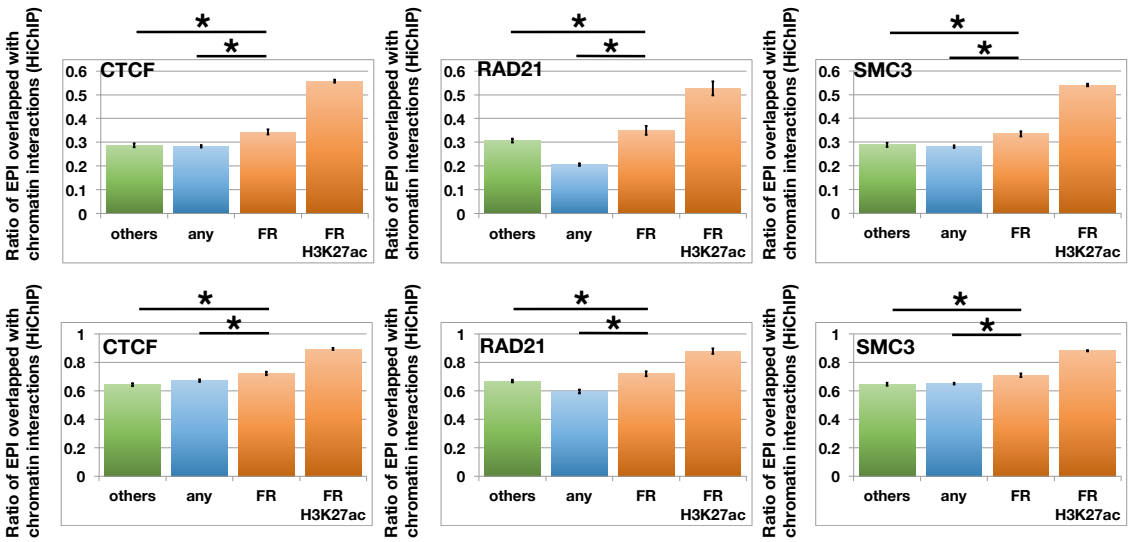

754

755 **Figure 3.** Comparison of enhancer-promoter interactions (EPI) with chromatin
756 interactions in T cells. EPI were predicted based on enhancer-promoter association
757 (EPA) shortened at the genomic locations of biased orientation of DNA binding motif
758 sequence of a transcription factor. Total 136 biased orientation (70 FR and 73 RF) of
759 DNA motif sequences including CTCF and cohesin showed a significantly higher ratio
760 of EPI overlapped with three replications of HiChIP chromatin interactions respectively
761 than the other types of EPAs in T cells. The upper part of the figure is a comparison of
762 EPI with HiChIP chromatin interactions with more than 6,000 counts for each
763 interaction, and the lower part of the figure is a comparison of EPI with HiChIP
764 chromatin interactions with more than 1,000 counts for each interaction. FR:
765 forward-reverse orientation of DNA motif. any: any orientation (i.e. without considering
766 orientation) of DNA motif. others: enhancer-promoter association not shortened at the
767 genomic locations of DNA motif. FR H3K27ac: EPI were predicted using DNA motif
768 in open chromatin regions overlapped with H3K27ac histone modification marks. *

769 *p*-value < 10^{-9}.

770

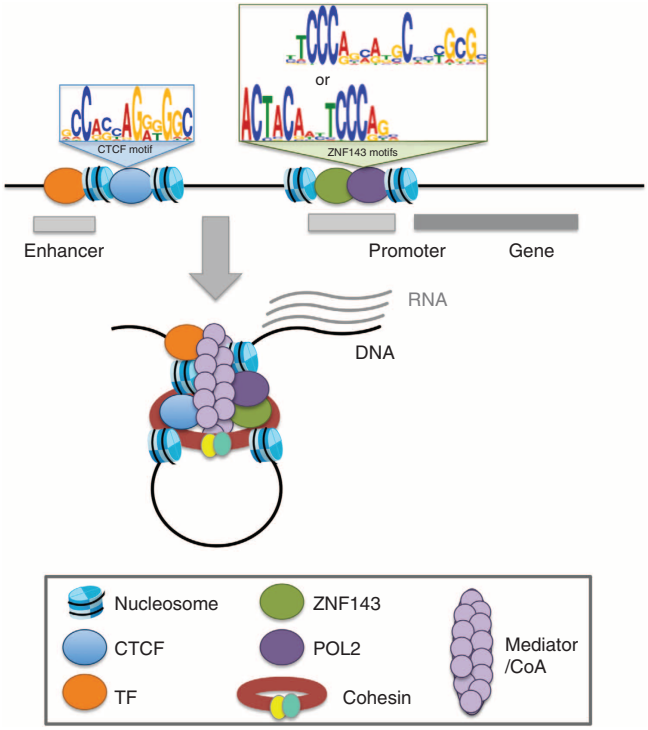

771

772 **Figure 4.** Schematic representation of chromatin interactions involving gene promoters.

773 ZNF143 contributes the formation of chromatin interactions by directly binding the

774 promoter of genes establishing looping with distal element bound by CTCF (Bailey et al.

775 2015).

776

Tables

Table 1. Top 90 biased orientation of DNA binding motif sequences of transcription factors in monocytes. TF: DNA binding motif sequences of transcription factors. Score: $-\log_{10}$ (*p*-value).

Forward-reverse orientation

TF	Score	TF	Score	TF	Score
SRF	74.05	EVI1	37.37	PAX5	28.42
YY1	71.30	ELK1:PAX1	36.54	RUNX2	27.95
ZNF658	70.76	RFX2	36.34	AP1	27.62
IRF7	65.05	SP2	36.15	ZNF836	27.60
PHYPADRAFT	63.98	ELF2	35.92	IRF	27.56
ESE3	60.18	NFIC	34.36	NR2F2	27.44
GCM1:CEBPB	58.35	HSF2	34.27	NR2C2	27.02
STAT1	55.66	KLF14	33.83	IKZF1	26.87
STA5A	54.84	ZF5	33.79	ESR2	26.64
RAD21	54.11	FXR	33.36	HIC1	26.58
TFE2	53.78	EPAS1	33.08	RREB1	26.56
ZNF623	53.59	USF	33.07	TCF12	26.29
ZNF317	52.78	ZNF646	32.47	FOS:JUN	26.07
ZNF93	52.13	ERR1	32.30	CMYB	25.86
CTCFL	50.49	NEUROD1	32.08	NKX61	25.41
HMBOX1	49.33	E2F8	31.95	TFAP2A	25.40
CTCF	47.24	ZNF660	31.55	NR4A3	25.37
ZKSC3	46.61	ZN219	31.45	ZNF709	25.15
STAT4	45.64	TCFAP2C	31.08	GTF3C2	25.04
E2F	45.63	MYB	30.93	SMAD5	24.40
SMAD2:SMAD3:SMAD4	43.91	HOXD12:ELK1	30.47	WT1	24.19
ABR1	43.81	THAP1	30.20	HIC2	24.16
P53	40.09	GATA1	30.17	ZNF695	24.07
BPTF	39.06	STAT3	29.85	ZSC31	23.98
RFX5	38.00	MXI1	29.73	GLIS1	23.79
HME1	37.88	SOX10	29.57	TCF3	23.55
NR1I2	37.70	HAT5	29.56	ZNF284	23.53
KLF1	37.61	PURA	29.03	PGAM2	23.44
AT4G28140	37.47	SMC3	28.59	ZFP82	23.35
ZKSCAN1	37.45	NFYB	28.50	ZNF214	23.32

Reverse-forward orientation

TF	Score	TF	Score	TF	Score
HNF1B	77.23	FOXI1	37.39	MSX2	26.00
STAT4	73.89	RARA	36.47	HOXC8	25.97
ZNF28	71.72	ZNF195	35.51	RXRA	25.45
TF7L1	67.52	ZNF449	34.50	MYOG	25.21
ZNF225	61.87	DOBOX5	34.48	SMAD4	25.15
CTCF	53.54	LEF1	33.87	PO3F2	24.99
STAT3	53.06	CETS2	33.69	IRF4	24.96
STAT5A	52.61	E2F3	33.22	ZNF233	24.53
PAX5	52.10	NKX3	33.07	RFX3	24.45
SRF	51.83	RBPJ	32.95	LDSPOLYA	23.76
ZNF670	50.69	SP1	32.79	ZNF682	23.56
ETV7	50.48	ZNF524	32.31	RXRB	23.34
TEL1	49.47	CDX2	32.10	EVI1	23.14
BCL6	49.19	TFAP4:ETV1	31.94	ETS2	22.98
ETV6	48.78	SOX2	30.80	OBOX2	22.95
NFY	47.73	SOX9	30.72	ZNF770	22.85
ZNF286B	46.85	PRDM1	30.66	ERG	22.75
ZFP82	46.84	CD59	29.85	TCF3	22.67
ZNF343	45.78	SOX11	29.34	IRF1	22.44
ZNF681	45.36	ZN320	28.86	TAACC	22.31
STAT5B	44.72	MYC	28.58	ZNF687	22.26
KLF16	44.33	ZNF316	28.34	IRF3	22.13
HNF4A	42.24	NR2F1	28.34	NRSE	21.97
P73	41.49	ZNF121	28.26	P53	21.92
EOMES	40.45	HOXB2:NHLH1	28.18	TCFAP2B	21.78
WT1	40.11	E2F2	27.94	AHR	21.40
BCL3	39.66	BDP1	27.63	ZFP641	20.09
SP8	38.96	HSF1	27.03	NRF3	19.94
TEAD1	38.73	ZBTB2	26.79	ZNF76	19.81
E2F4	37.67	SPI1	26.15	BRF2	19.77

Table 2. Top 30 forward-reverse orientation of DNA binding motif sequences of transcription factors in HUVEC and MCF-7 cells. TF: DNA binding motif sequences of transcription factors. Score: $-\log_{10}$ (p-value).

HUVEC

TF	Score
PAX5	19.30
TBX5	14.60
NANOG	12.98
BATF	11.52
HNF1A	10.94
THAP1	10.45
NR2C2	9.67
SULT1A2	9.67
CTCF	9.50
RAD21	9.01
COT2	6.84
MYB	6.18
EKLF	6.17
PIF7	5.95
ZNF695	5.90
SMAD5	5.70
TCFAP2A	5.52
YY1	5.50
YBX1	5.37
CMYB	5.26
HME1	5.07
TCF12	5.06
TFAP2A	4.83
HNF4A	4.36
SMC3	4.20
RXRA:VDR	3.64
P53	3.60
STA5A	3.40
STAT4	3.36
ZNF71	2.93

MCF-7

TF	Score
E2F6	57.73
EGR1	48.41
ABR1	34.79
CACBINDINGPROTEIN	28.34
KLF16	28.16
RREB1	25.42
PO4F1	24.64
ZN219	23.13
SP1	22.41
SP2	21.88
KLF15	21.33
ZNF521	21.05
CTCF	20.02
ESE3	19.92
ZNF143	17.47
FOXP1	16.99
GTF2I	16.32
ERF9	15.59
TF3A	15.51
TCF3	14.03
HIC2	13.94
GKLF	13.80
CXXC1	13.75
SMC3	12.91
CTCFL	12.67
RAD21	12.00
STA5B	11.94
STAT1	11.78
KLF12	11.57
SP4	11.20

Table 3. Biased orientation of repeat DNA sequences in monocytes. Score: $-\log_{10}$ (p-value).

Forward-reverse (FR) orientation (using H3K27ac histone modification marks)

Repeat DNA seq.	Score
MLT1F1	6.75

Reverse-forward (RF) orientation

Repeat DNA seq.	Score
LTR16C	69.39
L1ME4b	23.90
AluSg	23.61

Table 4. Top 30 of co-locations of biased orientation of DNA binding motif sequences of transcription factors in monocytes. Co-locations of DNA motif sequence of CTCF with another biased orientation of DNA motif sequence were shown in a separate table. Motif 1,2: DNA binding motif sequences of transcription factors. # both: the number of open chromatin regions including both Motif 1 and Motif 2. # motif 1: the number of open chromatin regions including Motif 1. # motif 2: the number of open chromatin regions including Motif 2. # others: the number of open chromatin regions not including Motif 1 and Motif 2. Open chromatin regions overlapped with histone modification marks (H3K27ac) were used (Total 26,095 regions).

Motif 1	Motif 2	# both	# motif 1	# motif 2	# others	*p*-value
MAZ	RREB1	7506	809	1770	16010	0
KLF5	MAZ	7181	1151	2095	15668	0
KLF13	MAZ	7128	881	2148	15938	0
MAZ	ZN148	7079	1027	2197	15792	0
MAZ	PATZ1	6931	1088	2345	15731	0
CDA7L	MAZ	6837	1050	2439	15769	0
KLF13	RREB1	6802	1513	1207	16573	0
MAZ	SP1	6698	811	2578	16008	0
CDA7L	KLF5	6668	1219	1664	16544	0
KLF5	ZN148	6644	1688	1462	16301	0
KLF11	MAZ	6548	802	2728	16017	0
PATZ1	RREB1	6538	1777	1481	16299	0
RREB1	ZN148	6521	1794	1585	16195	0
KLF11	KLF5	6446	904	1886	16859	0
MAZ	WT1	6444	1005	2832	15814	0
KLF5	SP1	6337	1995	1172	16591	0
CDA7L	ZN148	6313	1574	1793	16415	0
MAZ	SMAD2	6297	1168	2979	15651	0
SP1	ZN148	6292	1217	1814	16772	0
KLF5	SMAD2	6281	2051	1184	16579	0
CDA7L	KLF11	6232	1655	1118	17090	0
RREB1	SP1	6219	2096	1290	16490	0
WT1	ZN148	6205	1901	1244	16745	0
PATZ1	WT1	6145	1874	1304	16772	0
RREB1	WT1	6103	2212	1346	16434	0
KLF13	SP1	6084	1425	1925	16661	0
CDA7L	SP1	6051	1836	1458	16750	0
CDA7L	SMAD2	6034	1853	1431	16777	0
KLF11	RREB1	6034	1316	2231	16514	0
KLF11	ZN148	6030	1320	2076	16669	0

Motif 1	Motif 2	# both	# motif 1	# motif 2	# others	*p*-value
CTCF	MAZ	3371	671	5905	16148	0
CTCF	KLF5	3344	698	4988	17065	0
CTCF	RREB1	3126	741	5189	17039	0
CTCF	RAD21	2456	1586	166	21887	0
CTCF	CTCFL	1519	137	1078	23361	0
CTCF	RXRA	1459	336	1641	22659	0
CTCF	SMC3	1036	170	1561	23328	0
CTCFL	MAZ	2462	469	6814	16350	0
CTCFL	KLF5	2351	5981	580	17183	0
CTCFL	RAD21	1371	285	433	24006	0
CDA7L	CTCF	3238	4649	804	17404	0

819 **Table 5.** Comparison of enhancer-promoter interactions (EPI) with chromatin
820 interactions in T cells. The upper tables show the number of biased orientation of DNA
821 motifs, where a significantly higher ratio of EPI, which were predicted based on
822 enhancer-promoter association (EPA) (iii), overlapped with HiChIP chromatin
823 interaction data than the other types of EPA (i) and (ii). The middle tables show the 70
824 FR and 73 RF orientations of DNA motifs found in common among B2T1, B2T2 and
825 B3T1 replications in the upper table. The lower table shows that among 43 biased
826 orientation of DNA motifs found in both monocytes and T cell, 31 were matched with
827 the analysis of HiChIP for three types of EPA. TF: DNA binding motif sequence of a
828 transcription factor. Score: $-\log_{10}$ (*p*-value). Inf: *p*-value = 0. Score 1: Comparison of
829 EPA shortened at the genomic locations of FR or RF orientation of DNA motif
830 sequence [EPA (iii)] with EPA not shortened [EPA (i)]. Score 2: Comparison of EPA
831 shortened at the genomic locations of FR or RF orientation of DNA motif sequence
832 [EPA (iii)] with EPA shortened at the genomic locations of any orientation of DNA
833 motif sequence [EPA (ii)].

1. Comparison of EPI with HiChIP data among three EPA (i), (ii) and (iii)

Replication of HiChIP data	Total no. (FR + RF) of DNA motifs	No. of FR DNA motifs	No. of RF DNA motifs
B2T1	165	86	90
B2T2	168	85	92
B3T1	189	96	105
DNA motifs found in common among replications			
B2T1 and B2T2	148	75	81
B2T1 and B3T1	148	48	81
B2T2 and B3T1	147	76	79
B2T1, B2T2 and B3T1	136	70	73

2. Comparison of EPI with HiChIP data between two EPA (i) and (iii)

Replication of HiChIP data	Total no. (FR + RF) of DNA motifs	No. of FR DNA motifs	No. of RF DNA motifs
B2T1	358	195	201
B2T2	360	196	203
B3T1	365	195	209
DNA motifs found in common among replications			
B2T1 and B2T2	357	195	200
B2T1 and B3T1	357	194	201
B2T2 and B3T1	358	194	203
B2T1, B2T2 and B3T1	356	194	200

Forward-reverse (FR) orientation

TF	Score 1	Score 2
ABL1	120.20	4.48
AP2GAMMA	64.98	6.76
BATF	104.50	2.89
BC11A	114.77	4.72
CDC5L	46.20	12.32
CEBPG	113.24	8.73
CHOP	323.31	2.83
CTCF	109.95	16.53
CTCFL	89.06	16.88
CXXC1	98.89	10.97
DEC1	105.31	6.77
EGR1	129.00	12.41
EGR2	97.63	3.69
EGR3	105.43	4.92
EKLF	98.41	10.61
ELF5	114.76	3.90
ER71	246.20	2.48
ERF:EOMES	323.31	15.05
ETV4	206.76	7.18
FOXA2	323.31	3.48
FOXO3	323.31	3.71
GABPBETA	187.48	4.43
GATA5	176.92	1.89
GFI1	323.31	10.70
GFI1B	252.86	12.43
HIC1	99.40	1.96
HMGA2	322.83	7.48
INSM2	323.31	2.54
JUN	184.60	16.41
JUNB	158.94	2.57
KLF1	188.04	1.92
LHX8	323.31	3.39
MAF	136.76	6.56
MAFK	42.30	2.43
MYBB	253.52	8.74

TF	Score 1	Score 2
NFAC2	102.90	10.64
NFAC3	117.02	2.13
NFAC4	129.06	11.87
NFAT5	169.03	10.79
P50:P50	147.45	6.59
PRDM6	243.21	13.67
RAD21	98.81	10.93
REL	100.28	8.06
RFX5	138.49	2.53
RREB	98.91	4.13
RXRA	99.72	3.24
SIN3A	39.49	6.17
SMC3	78.49	20.74
SMRC2	106.88	8.79
SNF5	69.86	2.27
SP5	58.99	5.59
SRP9	147.33	2.92
STAF	201.83	9.43
SUZ12	102.37	7.25
TAL1	109.90	13.57
TF65	118.80	4.02
VEZF1	43.90	3.26
YBOX1	91.34	4.41
YBX1	165.05	4.58
ZBP89	82.45	6.26
ZBRK1	323.31	4.03
ZBT16	157.35	20.95
ZN263	63.43	8.19
ZNF227	323.31	3.42
ZNF253	Inf	18.36
ZNF331	120.46	2.13
ZNF585A	179.25	8.49
ZNF681	Inf	35.47
ZNF721	148.23	3.75
ZNF846	Inf	11.20

Reverse-forward (RF) orientation

TF	Score 1	Score 2
AML3	94.46	2.21
AP1	71.45	6.80
ARI5B	57.76	2.72
CFOS	121.76	12.76
CFOS:CJUN	194.70	21.29
CHD2	76.76	2.22
CREB3	166.87	18.45
CREM	323.31	6.89
CTCF	74.93	18.84
CTCFL	60.12	12.79
DBP	263.45	5.42
E2F1	122.59	4.07
EFC	323.31	4.05
EGR1	263.41	5.42
EGR4	102.64	2.88
ELF2	95.04	3.38
ELF5	279.29	1.66
EP300	82.68	3.97
ETV2:PAX5	323.31	6.03
FOSB	146.18	14.44
FOSL1	137.95	13.98
FOXA	323.31	7.27
FOXA1	323.31	9.93
FOXO3A	323.31	6.53
GATA	209.11	8.22
GCM2:EOMES	56.33	4.61
GFI1	123.54	4.62
GFI1B	323.31	5.94
HSF1	44.39	3.11
HSF2	144.04	5.18
HXB1	323.31	3.91
HXB6	323.31	5.57
IKZF1	65.38	6.13
JUN:FOSB	77.62	2.75
JUN:JUNB	126.45	3.73
LYL1	74.51	2.65
MTF1	303.27	1.86

TF	Score 1	Score 2
MZF1	100.14	3.15
NKX2-1	323.31	7.34
NKX2-4	Inf	5.82
NKX2-5	323.31	4.23
P50	185.48	10.77
P53	71.49	6.47
P73	172.99	8.20
PKNX1	111.56	2.61
POU2F1:ELK1	323.31	4.66
RELA	306.11	4.11
RP58	210.42	3.73
RREB1	128.85	2.05
RXRB	57.75	2.29
SALL4	100.01	13.24
SIX6	96.78	11.15
TCF3	220.95	6.37
TCF4	64.91	2.34
TCFE2A	212.46	6.00
TF7L2	120.84	3.14
XBP1	105.73	2.57
ZBTB4	323.31	5.23
ZFP2	Inf	5.32
ZNF134	53.47	1.70
ZNF16	243.81	3.54
ZNF260	98.46	2.69
ZNF28	323.31	4.61
ZNF282	126.15	5.08
ZNF341	109.16	4.93
ZNF468	105.25	2.85
ZNF484	Inf	12.66
ZNF542P	244.54	5.52
ZNF580	78.41	2.95
ZNF625	Inf	6.14
ZNF714	39.80	3.57
ZNF721	111.46	4.37
ZNF837	87.54	1.74

TF	Score 1	Score 2
BATF	104.50	2.89
CTCF	109.95	16.53
CTCFL	89.06	16.88
CXXC1	98.89	10.97
EGR1	129.00	12.41
EKLF	98.41	10.61
ELF5	114.76	3.90
EP300	82.68	3.97
ETV4	206.76	7.18
FOSL1	137.95	13.98
GFI1	323.31	10.70
HIC1	99.40	1.96
HSF1	44.39	3.11
HSF2	144.04	5.18
KLF1	188.04	1.92
MAFK	42.30	2.43
MYBB	253.52	8.74
P53	71.49	6.47
P73	172.99	8.20
RAD21	98.81	10.93
RFX5	138.49	2.53
RREB1	98.91	4.13
RXRA	99.72	3.24
RXRB	57.75	2.29
SMC3	78.49	20.74
TAL1	109.90	13.57
TCF3	220.95	6.37
TF65	118.80	4.02
YBX1	165.05	4.58
ZNF28	323.31	4.61
ZNF721	111.46	4.37

841 **References**

842

843 Bailey SD, Zhang X, Desai K, Aid M, Corradin O, Cowper-Sal Lari R, Akhtar-Zaidi B,
844 Scacheri PC, Haibe-Kains B, Lupien M. 2015. ZNF143 provides sequence
845 specificity to secure chromatin interactions at gene promoters. *Nat Commun* **2**:
846 6186.
847 Bailey TL, Boden M, Buske FA, Frith M, Grant CE, Clementi L, Ren J, Li WW, Noble
848 WS. 2009. MEME SUITE: tools for motif discovery and searching. *Nucleic*
849 *acids research* **37**: W202-208.
850 Barutcu AR, Lajoie BR, Fritz AJ, McCord RP, Nickerson JA, van Wijnen AJ, Lian JB,
851 Stein JL, Dekker J, Stein GS et al. 2016. SMARCA4 regulates gene expression
852 and higher-order chromatin structure in proliferating mammary epithelial cells.
853 *Genome research* **26**: 1188-1201.
854 Bejerano G, Lowe CB, Ahituv N, King B, Siepel A, Salama SR, Rubin EM, Kent WJ,
855 Haussler D. 2006. A distal enhancer and an ultraconserved exon are derived
856 from a novel retroposon. *Nature* **441**: 87-90.
857 Chen M, Manley JL. 2009. Mechanisms of alternative splicing regulation: insights from
858 molecular and genomics approaches. *Nat Rev Mol Cell Biol* **10**: 741-754.
859 Das D, Clark TA, Schweitzer A, Yamamoto M, Marr H, Arribere J, Minovitsky S,
860 Poliakov A, Dubchak I, Blume JE et al. 2007. A correlation with exon
861 expression approach to identify cis-regulatory elements for tissue-specific
862 alternative splicing. *Nucleic acids research* **35**: 4845-4857.
863 de Souza FS, Franchini LF, Rubinstein M. 2013. Exaptation of transposable elements
864 into novel cis-regulatory elements: is the evidence always strong? *Mol Biol Evol*
865 **30**: 1239-1251.
866 de Wit E, Vos ES, Holwerda SJ, Valdes-Quezada C, Verstegen MJ, Teunissen H,
867 Splinter E, Wijchers PJ, Krijger PH, de Laat W. 2015. CTCF Binding Polarity
868 Determines Chromatin Looping. *Molecular cell* **60**: 676-684.
869 Grant CE, Bailey TL, Noble WS. 2011. FIMO: scanning for occurrences of a given
870 motif. *Bioinformatics (Oxford, England)* **27**: 1017-1018.
871 Guo Y, Xu Q, Canzio D, Shou J, Li J, Gorkin DU, Jung I, Wu H, Zhai Y, Tang Y et al.
872 2015. CRISPR Inversion of CTCF Sites Alters Genome Topology and

873 Enhancer/Promoter Function. *Cell* **162**: 900-910.
874 Javierre BM, Burren OS, Wilder SP, Kreuzhuber R, Hill SM, Sewitz S, Cairns J,
875 Wingett SW, Varnai C, Thiecke MJ et al. 2016. Lineage-Specific Genome
876 Architecture Links Enhancers and Non-coding Disease Variants to Target Gene
877 Promoters. *Cell* **167**: 1369-1384 e1319.
878 Jeong M, Huang X, Zhang X, Su J, Shamim M, Bochkov I, Reyes J, Jung H, Heikamp
879 E, Presser Aiden A et al. 2017. A Cell Type-Specific Class of Chromatin Loops
880 Anchored at Large DNA Methylation Nadirs. *bioRxiv*.
881 Ji X, Dadon DB, Abraham BJ, Lee TI, Jaenisch R, Bradner JE, Young RA. 2015.
882 Chromatin proteomic profiling reveals novel proteins associated with
883 histone-marked genomic regions. *Proc Natl Acad Sci U S A* **112**: 3841-3846.
884 Jin C, Kato K, Chimura T, Yamasaki T, Nakade K, Murata T, Li H, Pan J, Zhao M, Sun
885 K et al. 2006. Regulation of histone acetylation and nucleosome assembly by
886 transcription factor JDP2. *Nat Struct Mol Biol* **13**: 331-338.
887 Jjingo D, Conley AB, Wang J, Marino-Ramirez L, Lunyak VV, Jordan IK. 2014.
888 Mammalian-wide interspersed repeat (MIR)-derived enhancers and the
889 regulation of human gene expression. *Mob DNA* **5**: 14.
890 John S, Sabo PJ, Thurman RE, Sung MH, Biddie SC, Johnson TA, Hager GL,
891 Stamatoyannopoulos JA. 2011. Chromatin accessibility pre-determines
892 glucocorticoid receptor binding patterns. *Nature genetics* **43**: 264-268.
893 Jolma A, Yan J, Whitington T, Toivonen J, Nitta KR, Rastas P, Morgunova E, Enge M,
894 Taipale M, Wei G et al. 2013. DNA-binding specificities of human transcription
895 factors. *Cell* **152**: 327-339.
896 Karolchik D, Barber GP, Casper J, Clawson H, Cline MS, Diekhans M, Dreszer TR,
897 Fujita PA, Guruvadoo L, Haeussler M et al. 2014. The UCSC Genome Browser
898 database: 2014 update. *Nucleic acids research* **42**: D764-770.
899 Katainen R, Dave K, Pitkanen E, Palin K, Kivioja T, Valimaki N, Gylfe AE,
900 Ristolainen H, Hanninen UA, Cajuso T et al. 2015. CTCF/cohesin-binding sites
901 are frequently mutated in cancer. *Nature genetics* **47**: 818-821.
902 Kheradpour P, Kellis M. 2014. Systematic discovery and characterization of regulatory
903 motifs in ENCODE TF binding experiments. *Nucleic acids research* **42**:
904 2976-2987.
905 Kulakovskiy IV, Vorontsov IE, Yevshin IS, Sharipov RN, Fedorova AD, Rumynskiy EI,

906 Medvedeva YA, Magana-Mora A, Bajic VB, Papatsenko DA et al. 2018.
907 HOCOMOCO: towards a complete collection of transcription factor binding
908 models for human and mouse via large-scale ChIP-Seq analysis. *Nucleic acids*
909 *research* **46**: D252-D259.
910 Li H, Durbin R. 2009. Fast and accurate short read alignment with Burrows-Wheeler
911 transform. *Bioinformatics (Oxford, England)* **25**: 1754-1760.
912 Li H, Handsaker B, Wysoker A, Fennell T, Ruan J, Homer N, Marth G, Abecasis G,
913 Durbin R, Genome Project Data Processing S. 2009. The Sequence
914 Alignment/Map format and SAMtools. *Bioinformatics (Oxford, England)* **25**:
915 2078-2079.
916 McLean CY, Bristor D, Hiller M, Clarke SL, Schaar BT, Lowe CB, Wenger AM,
917 Bejerano G. 2010. GREAT improves functional interpretation of cis-regulatory
918 regions. *Nature biotechnology* **28**: 495-501.
919 Mumbach MR, Satpathy AT, Boyle EA, Dai C, Gowen BG, Cho SW, Nguyen ML,
920 Rubin AJ, Granja JM, Kazane KR et al. 2017. Enhancer connectome in primary
921 human cells identifies target genes of disease-associated DNA elements. *Nature*
922 *genetics* **49**: 1602-1612.
923 Newburger DE, Bulyk ML. 2009. UniPROBE: an online database of protein binding
924 microarray data on protein-DNA interactions. *Nucleic acids research* **37**:
925 D77-82.
926 Osato N. 2018. Characteristics of functional enrichment and gene expression level of
927 human putative transcriptional target genes. *BMC Genomics* **19**: 957.
928 Phanstiel DH, Van Bortle K, Spacek D, Hess GT, Shamim MS, Machol I, Love MI,
929 Aiden EL, Bassik MC, Snyder MP. 2017. Static and Dynamic DNA Loops form
930 AP-1-Bound Activation Hubs during Macrophage Development. *Molecular cell*
931 **67**: 1037-1048.e1036.
932 Portales-Casamar E, Thongjuea S, Kwon AT, Arenillas D, Zhao X, Valen E, Yusuf D,
933 Lenhard B, Wasserman WW, Sandelin A. 2010. JASPAR 2010: the greatly
934 expanded open-access database of transcription factor binding profiles. *Nucleic*
935 *acids research* **38**: D105-110.
936 Ramani V, Cusanovich DA, Hause RJ, Ma W, Qiu R, Deng X, Blau CA, Disteche CM,
937 Noble WS, Shendure J et al. 2016. Mapping 3D genome architecture through in
938 situ DNase Hi-C. *Nat Protoc* **11**: 2104-2121.

939 Rao SS, Huntley MH, Durand NC, Stamenova EK, Bochkov ID, Robinson JT, Sanborn
940 AL, Machol I, Omer AD, Lander ES et al. 2014. A 3D map of the human
941 genome at kilobase resolution reveals principles of chromatin looping. *Cell* **159**:
942 1665-1680.
943 Rebollo R, Romanish MT, Mager DL. 2012. Transposable elements: an abundant and
944 natural source of regulatory sequences for host genes. *Annu Rev Genet* **46**:
945 21-42.
946 Schreiber J, Libbrecht M, Bilmes J, Noble W. 2017. Nucleotide sequence and DNaseI
947 sensitivity are predictive of 3D chromatin architecture. *bioRxiv*.
948 Shannon P, Markiel A, Ozier O, Baliga NS, Wang JT, Ramage D, Amin N,
949 Schwikowski B, Ideker T. 2003. Cytoscape: a software environment for
950 integrated models of biomolecular interaction networks. *Genome research* **13**:
951 2498-2504.
952 Tabuchi TM, Deplancke B, Osato N, Zhu LJ, Barrasa MI, Harrison MM, Horvitz HR,
953 Walhout AJ, Hagstrom KA. 2011. Chromosome-biased binding and gene
954 regulation by the Caenorhabditis elegans DRM complex. *PLoS Genet* **7**:
955 e1002074.
956 Wang ET, Sandberg R, Luo S, Khrebtukova I, Zhang L, Mayr C, Kingsmore SF,
957 Schroth GP, Burge CB. 2008. Alternative isoform regulation in human tissue
958 transcriptomes. *Nature* **456**: 470-476.
959 Wang J, Vicente-Garcia C, Seruggia D, Molto E, Fernandez-Minan A, Neto A, Lee E,
960 Gomez-Skarmeta JL, Montoliu L, Lunyak VV et al. 2015. MIR retrotransposon
961 sequences provide insulators to the human genome. *Proc Natl Acad Sci U S A*
962 **112**: E4428-4437.
963 Wang L, Wang S, Li W. 2012. RSeQC: quality control of RNA-seq experiments.
964 *Bioinformatics (Oxford, England)* **28**: 2184-2185.
965 Weintraub AS, Li CH, Zamudio AV, Sigova AA, Hannett NM, Day DS, Abraham BJ,
966 Cohen MA, Nabet B, Buckley DL et al. 2017. YY1 Is a Structural Regulator of
967 Enhancer-Promoter Loops. *Cell* **171**: 1573-1588 e1528.
968 Wingender E, Dietze P, Karas H, Knuppel R. 1996. TRANSFAC: a database on
969 transcription factors and their DNA binding sites. *Nucleic acids research* **24**:
970 238-241.
971 Xie Z, Hu S, Blackshaw S, Zhu H, Qian J. 2010. hPDI: a database of experimental

972 human protein-DNA interactions. *Bioinformatics (Oxford, England)* **26**:
973 287-289.
974 Zhang H, Li F, Jia Y, Xu B, Zhang Y, Li X, Zhang Z. 2017. Characteristic arrangement
975 of nucleosomes is predictive of chromatin interactions at kilobase resolution.
976 *Nucleic acids research* **45**: 12739-12751.
977 Zhang Y, An L, Xu J, Zhang B, Zheng WJ, Hu M, Tang J, Yue F. 2018. Enhancing
978 Hi-C data resolution with deep convolutional neural network HiCPlus. *Nat*
979 *Commun* **9**: 750.
980 Zhao Y, Stormo GD. 2011. Quantitative analysis demonstrates most transcription
981 factors require only simple models of specificity. *Nature biotechnology* **29**:
982 480-483.
983